# Characterization of Aquifer System and Fulfilment of South-to-North Water Diversion Project in North China Plain Using Geodetic and Hydrological Data


**Mingjia Li[1], Jianbao Sun[2], Lian Xue[3], Zheng-Kang Shen[3,4]**

1, Department of Earth and Space Sciences, Southern University of Science and Technology, Shenzhen, China
2, State Key Lab. of Earthquake Dynamics, Institute of Geology, China Earthquake Administration, Beijing, China
3, School of Earth and Space Sciences, Peking University, Beijing, China
4, Department of Earth, Planetary, and Space Sciences, University of California, Los Angeles, CA, United States
Contact: Jianbao Sun (sunjianbao@ies.ac.cn)


## Introduction

Groundwater overexploitation and its resulting surface subsidence have been critical issues in the North China Plain (NCP) for the last half-century. This problem, however, is being alleviated by the implementation of the South-to-North Water Diversion (SNWD) Project since 2015. Here, we monitor surface deformation and investigate aquifer physical properties in NCP by combining Interferometric Synthetic Aperture Radar (InSAR), Global Positioning System (GPS), and hydraulic head data observed during 2015-2019.

## Objective

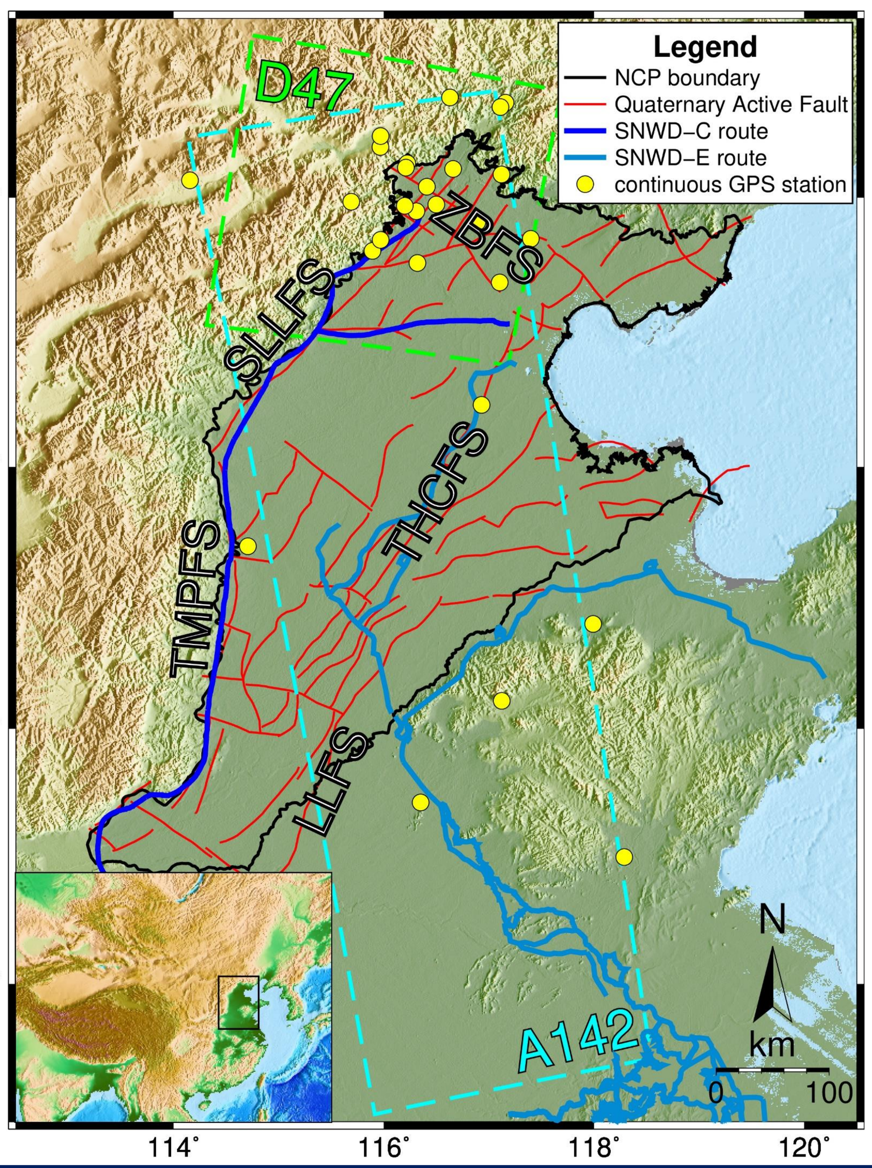


Figure 1. Tectonic setting of NCP. The black lines mark the boundary of NCP. The cyan dashed rectangle shows the imprint of ascending InSAR track 142, and the green one shows the imprint of descending InSAR track 47, whose data are used in this study. The light blue and dark blue lines represent the East and Central Routes of the SNWD Project. The yellow dots are the continuous GPS stations, which are used to establish a reference in the InSAR data processing. The red lines indicate the location of the Quaternary active faults. Fault name abbreviations: ZBFS, Zhangjiakou-Bohai fault system; LLFS, Liaocheng-Lankao fault system; THCFS, Tangshan-Hejian-Cixian fault system; SLLFS, Sanhe-Laishui-Lingshou fault system; TMPFS, Taihang Mountain Piedmont fault system.

## Data

We process 2 tracks of Synthetic Aperture Radar (SAR) data from the Sentinel-1A/1B satellites recorded between June 2015 and June 2019, including 92 ascending images of track 142 and 96 descending images of track 47. Interferograms are generated using the GAMMA software, and the InSAR time series are generated using the Stanford Method for Persistent Scatterer (StaMPS) software package. All of the interferograms are formed with one reference image per track.

Also, we acquire our GPS dataset from two separate sources: the Crustal Movement Observation Network of China (CMONOC) project and the Beijing Continuously Operating Reference Station (BJCORS) network, including 49 continuous and 432 campaign GPS stations. Moreover, we collect hydraulic head data on well water level from difference sources. After data integration, we finally get 197 stations with only confined aquifer observation, 124 stations with only unconfined aquifer observation, and 46 stations with both confined and unconfined aquifer observation.

## Method

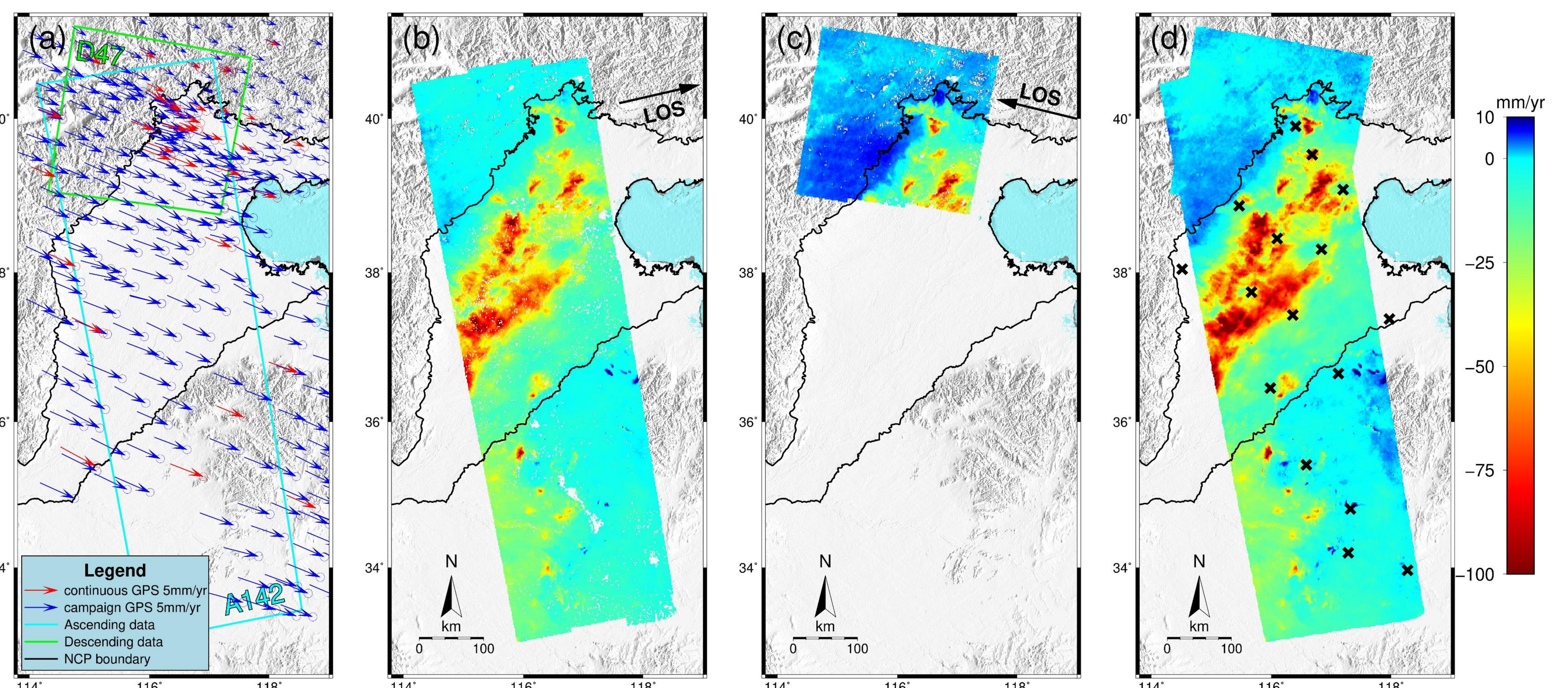


Figure 2. Surface deformation results. (a) Horizontal GPS velocity field. The red and blue arrows denote the velocities of the continuous and campaign GPS sites respectively. (b) Ascending track 142 mean LOS velocities. (c) Descending track 47 mean LOS velocities. (d) Derived vertical mean velocities. Black cross indicate the location of major cities in NCP.

In our research, we use Persistent Scatterer (PS) method to overcome the decorrelation problem, which is especially challenging in the vegetated and luxuriant NCP. Then we divide the study area into overlapping patches and use parallel computing algorithms, to reduce the computational load. Finally we successfully obtain the InSAR time series in NCP with full resolution for the first time and identify approximately $2 \times 10^6$ and $7 \times 10^5$ PS pixels for two tracks in our study area.

Here we use a combined atmosphere correction method, in which the first-order noise is estimated using the ERA5 global atmosphere model, and the residual noise is estimated using the Common Scene Stacking method. Then we synthesize InSAR and GPS time series data to correct for the long-wavelength noise in the InSAR data. Finally, based on the two tracks of InSAR time series data in LOS direction and continuous GPS time series data in horizontal direction, we can derive the surface deformation time series and mean velocity in vertical direction.

## Result

Surface vertical deformation can be caused by elastic (recoverable) and inelastic (unrecoverable) deformation. In this study, we use a sinusoidal function to fit the characteristic annual variation of deformation, and a second-order polynomial to fit the characteristic long-term deformation. The annual deformation signal is mostly elastic and recoverable, while the long-term deformation is mostly inelastic and unrecoverable:

$$D(t) = D_{seasonal}(t) + D_{long-term}(t) = Bsin(2\pi t) + Ccos(2\pi t) + K_0 + K_1 t + K_2 t^2$$

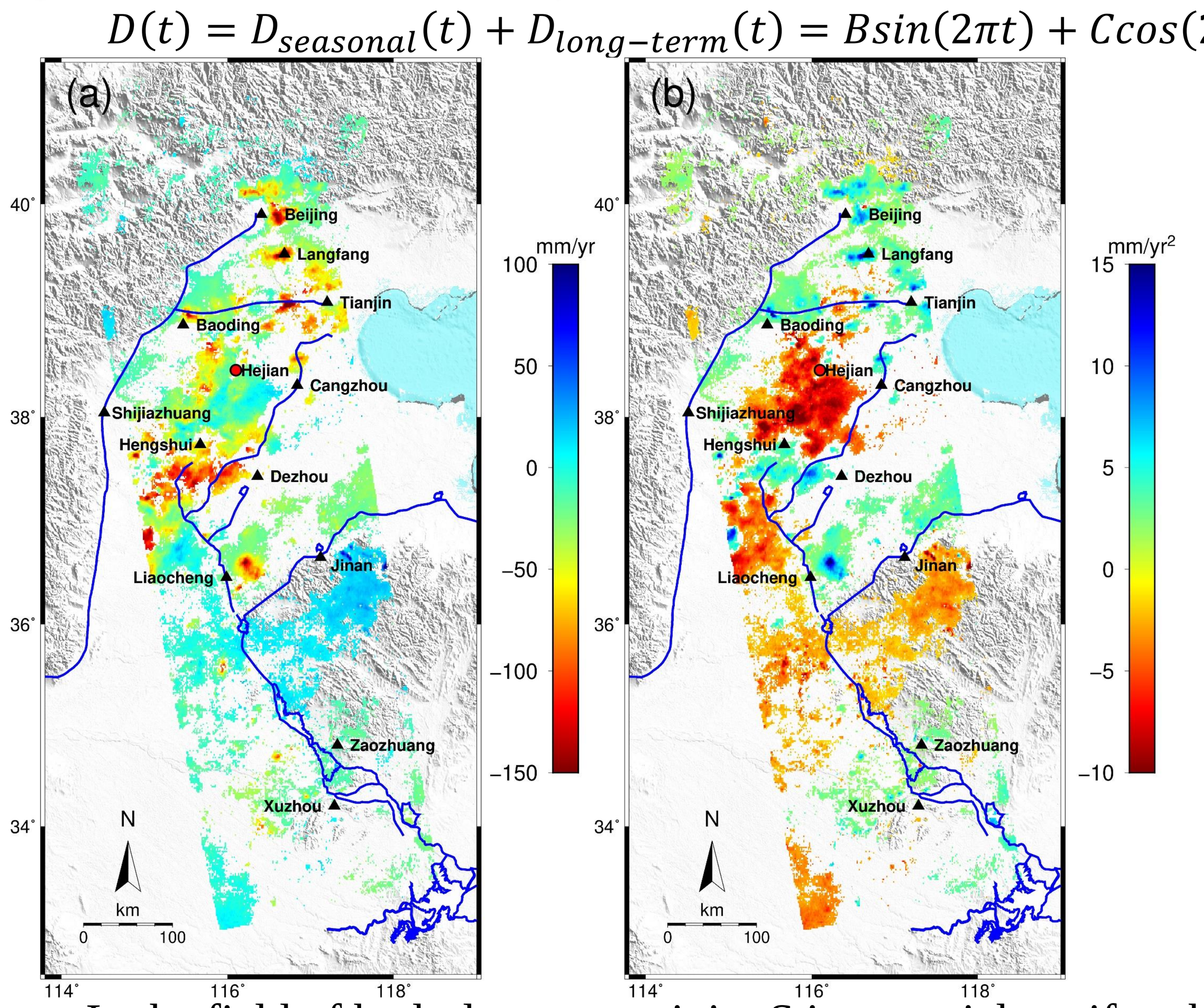


Figure 3. Spatial distribution of long-term (a) subsidence rate $K_1$ and (b) subsidence acceleration rate $K_2$. The area is determined by statistical F-test. The blue lines mark the aqueduct lines of the Central and East Routes of the SNWD Project. The black triangles mark the locations of major cities in NCP. We can see most of the areas where $K_2$ is positive are located along the aqueduct lines of the SNWD Project and are in and near the major cities along the lines.

In the field of hydrology, storativity S is a crucial aquifer physical property, which characterizes the capacity of an aquifer to store or release groundwater. In our research, using the seasonal deformation component and seasonal hydraulic confined and unconfined head change data, we can invert the storativity in NCP:

$$S = db/(dh_c - ndh_u)$$

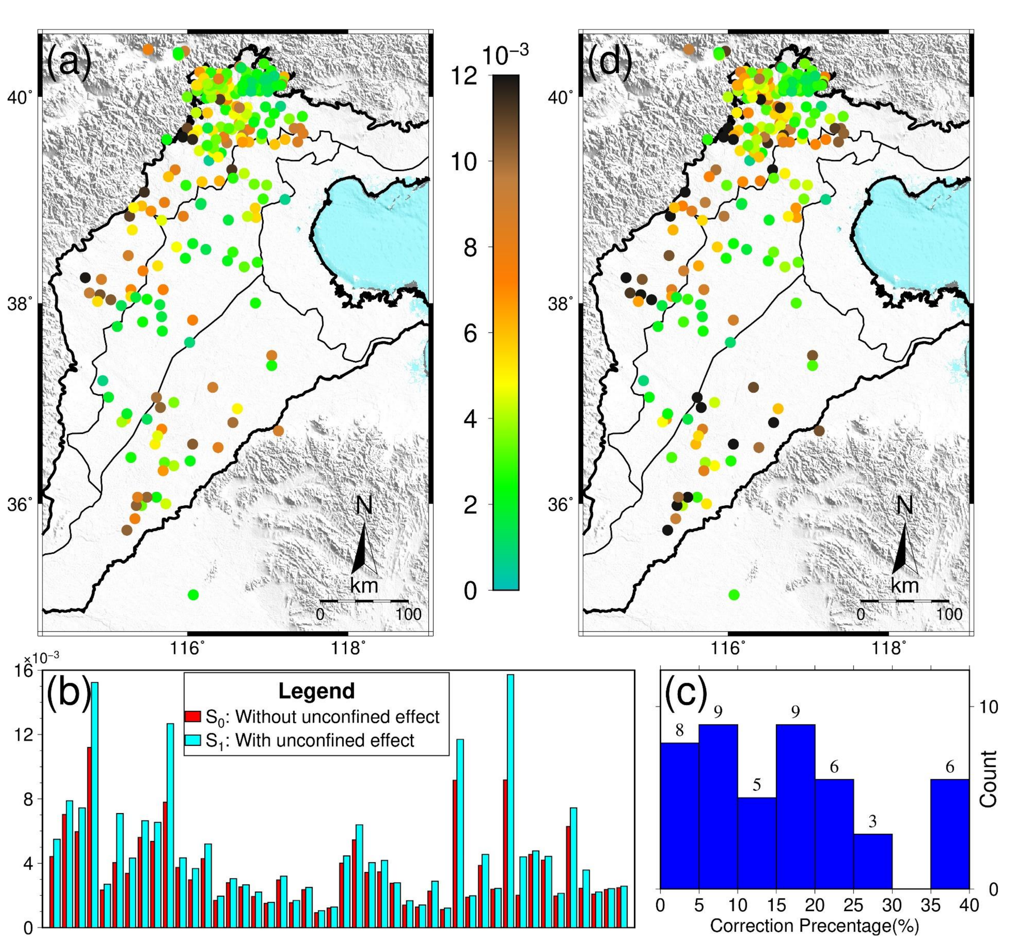


Figure 4. Comparison the storativity $S_0$ and $S_1$ for with and without unconfined aquifer effect. (a) Spatial distribution of $S_0$ (b) Comparison of storativity estimates and (c) correction percentage statistical distribution. (d) Spatial distribution of $S_1$.

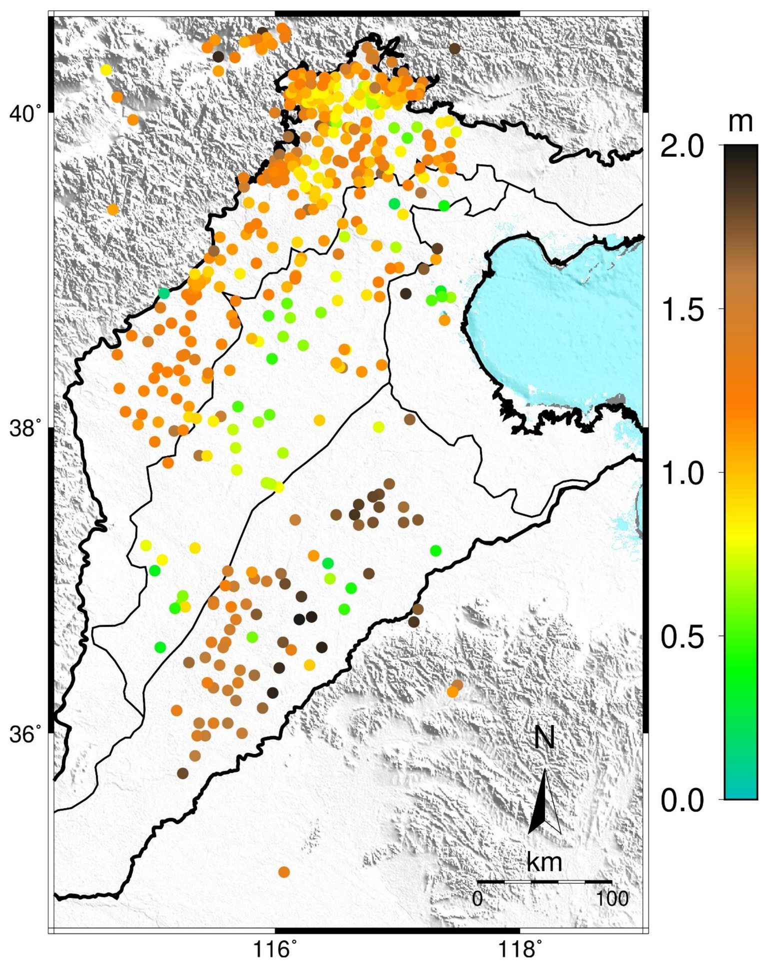

Figure 5. Thickness of clay lenses due to the time delay between seasonal signal of surface deformation and hydraulic head change.

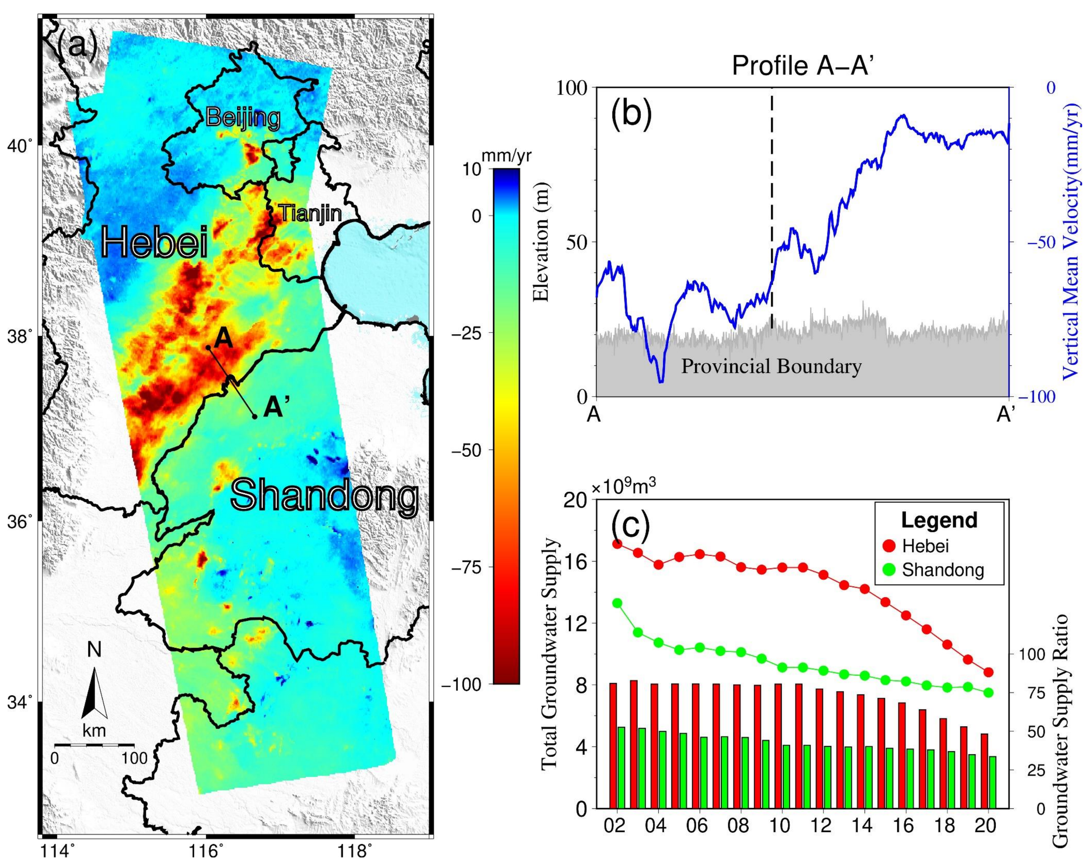


Figure 6. (a) Spatial distribution of vertical mean velocities and provincial administrative regions in NCP. Black thick lines mark the provincial boundaries and black thin line marks the A-A' profile. (b) The vertical mean velocity and elevation along the A-A' profile. (c) Statistics of annual total and ratio of the groundwater supply in the Hebei and Shandong Province. The difference in groundwater supply between two provinces makes a clear subsidence velocity difference along the province borderline.

## Conclusion

Using geodetic and hydrological data, we investigate the aquifer system and subsidence process and quantify the fulfillment of the SNWD Project on mitigating groundwater shortage in NCP. Geodetic observations reveal widespread and remarkable subsidence in the NCP, with an average rate of ~30 mm/yr, and ~100 mm/yr for the maximum. We successfully extract seasonal and long-term deformation components caused by different hydrogeological processes, and invert the storativity and thickness of clay lenses for the confined aquifer.

Our study also reveals fulfilment of the SNWD Project in alleviating the groundwater shortage, and demonstrates that the integration of geodetic and hydrological data can be effectively used for the assessment of groundwater circulation and to assist groundwater management and policy formulation.